CIVB Flashback Analysis with Simultaneous and Time Resolved PIV-LIF Measurements

Marco Konle, Anton Winkler, Frank Kiesewetter, Johann Wäsle, Thomas Sattelmayer

Lehrstuhl für Thermodynamik, Technische Universität München, Germany, konle@td.mw.tum.de

Abstract Combustion Induced Vortex Breakdown (CIVB) generating flame flashback in swirl burners was experimentally investigated. In the stable regime a bubble is created by the recirculation zone, which appears downstream of the combustor exit plane. Introduced by small changes of the flow field this bubble propagates upstream and transports the flame from the stable position inside the combustor into the premixing zone. To avoid this form of flashback and the damage of the upstream components due to overheating this phenomenon was investigated in detail. Previous experimental and numerical work identified the interaction of turbulence and chemistry as the root cause for CIVB and revealed that the vortex transport equation is well suited for the analysis of this interaction. Since the analysis showed that the position of the flame front with respect to the recirculation bubble governs the effects leading to CIVB this aspect was investigated in greater depth. In the experiment a premixed swirl burner without centerbody was investigated. The aerodynamic stabilization is realized with a properly tailored swirling main flow and an axial unswirled jet, which optimizes the vortex breakdown position. The experiments cover different burner geometries. Due to the high dynamics of the flame propagation during flashback High-Speed Particle Image Velocimetry (HS-PIV) and High-Speed Laser Induced Fluorescence (HS-LIF) were applied simultaneously to measure the dynamic change of the flow field and to track the flame front. In this framework the experimental investigations were focused on the tip of the bubble, which is the most relevant section for the onset of CIVB. The results of the experiments essentially confirm the mechanism derived from the analysis of earlier CFD data. In addition, instantaneous data is provided, which explains the observed strongly stochastic fluctuation of the flame tip before flashback due to CIVB occurs.

1. Introduction

Flame flashback deteriorates the reliability of premix burner systems, as flame propagation into the mixing zone overheats and damages the upstream hardware components. Since the reliability problems become more severe with increasing working pressure as well as air and flame temperature, the improvement of the understanding of the root causes of flashback has become an increasingly important task of combustion research. Three flashback types are known and well understood: If the turbulent flame speed is higher than the flow velocity flashback will occur in the bulk flow. The second kind of flashback, which propagates in the wall boundary layer against the main flow direction, will occur if the velocity gradient falls under a critical value. Furthermore, violent combustion instabilities can cause the sudden transition of the flame against the main flow direction into the premixing zone.

For the first time a fourth mechanism was explicitly observed during investigations of a swirl burner without center body by Fritz and Kröner (Fritz et al. 2004; Kröner et al. 2003; Kröner et al. 2005): *Combustion Induced Vortex Breakdown* (CIVB) differs substantially from the three other classical flashback types. When CIVB occurs, the sudden propagation of the flame from the combustor into the premix duct is observed. The effect was observed for several configurations, when the equivalence ratio was increased above a critical value or the mixture mass flow was reduced below a minimum. Figure 1 shows a sequence of frames taken from a OH*-chemiluminescence high-speed video taken during flame flashback. As the flame always propagates

on the centerline against the main flow direction, although the flow velocity was higher than the turbulent flame speed, the first and second type of flashback cannot be made responsible for the effect. Thermoacoustic instabilities causing flashback (third flashback type) did not occur in the experiments. Therefore, a fourth flashback type was identified in these studies. Fritz and Kröner also detected that CIVB prone and safe configurations exist. They showed that surprisingly small geometrical changes of the swirler were sufficient for making a stable configuration prone to CIVB driven flashback and vice versa. Based on numerical simulations (Kiesewetter et al. 2003; Kiesewetter 2005) the reasons for this type of flashback could be identified using a post-processing analysis of the CFD data, which delivered the distribution of vorticity and its source terms in the entire flow field. The same approach showed that the difference between CIVB safe and CIVB prone configurations is closely linked to the location of the flame front with respect to the tip of the recirculation bubble. The main purpose of the measurements presented below was the experimental validation of the conclusion drawn from the numerical work applying high-speed laser techniques to different configurations and fuel mixtures. In addition, the stochastic nature of the onset of CIVB was experimentally explored.

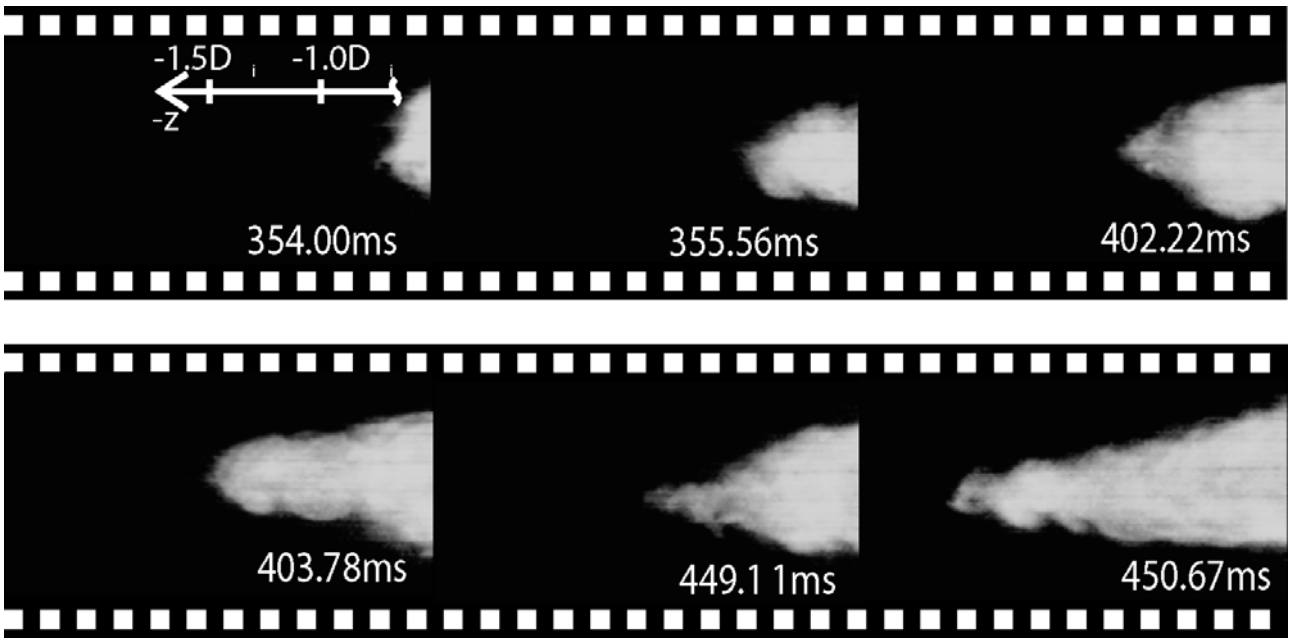

Fig. 1 Flame propagation during a CIVB driven flashback (Fritz et al. 2004).

After a short compilation of the theoretical background and the conclusions drawn from the numerical analysis in section 2, the setup, which is used in the verification experiment, will be presented in section 3. In section 4, the simultaneous and synchronized application of the two high-speed measurement techniques is described before the measurement results will be presented and analyzed in section 5.

2. Theory

Flows and their dynamics are usually modeled with the Navier-Stokes equations, but for the analysis of flashback the vortex transport equation is more suitable (Darmofal 1993), as it provides a direct access to the transport, generation and destruction of vorticity:

$$\frac{D\omega}{Dt} = \frac{\partial}{\partial t}(\vec{\omega}) + (\vec{U}\cdot\nabla)\vec{\omega} = (\vec{\omega}\cdot\nabla)\vec{U} - \vec{\omega}(\nabla\cdot\vec{U}) + \frac{1}{\rho^2}(\nabla\rho\times\nabla p) \qquad (1)$$

Equation (1) describes the inviscid transport of the vorticity ω. The vorticity generation is caused by stretching and tilting due to diverging streamlines, the first term on the right hand side, volume expansion due to heat release (second term) and baroclinic torque due to density gradients (third term). Contributions of viscous diffusion and dissipation (Hasegawa et al. 2001) are of minor influence and have been therefore neglected in equation (1). Diverging streamlines are produced near the burner exit plane. In this zone stretching and tilting induces changes of vorticity independently of the existence of a flame in the combustor. In contrast, the volume expansion and also the baroclinic torque do not exist in isothermal flows. They modify the vorticity budget only in cases with chemical reaction and with heat release causing density gradients and acceleration of the flow.

In the case of rotational symmetry, the generation of negative azimuthal vorticity induces axial velocity against the main flow direction according to the law of Biot-Savart (Panton 1996):

$$w_{ind} = \frac{1}{2}\int_{-\infty}^{\infty}\int_{0}^{\infty} \frac{r^{*2}\eta(r^*, z^*)}{[r^{*2} + (z - z^*)^2]^{\frac{3}{2}}} dr^* dz^* \qquad (2)$$

In normal operation of the burner vortex breakdown at the burner exit plane creates an internal recirculation zone (IRZ), which transports heat and active species upstream to the tip of the flame and provides aerodynamical flameholding. The induced velocity w_{ind} forms in this zone a recirculation bubble with a stagnation point at its upstream tip. The position and the contour of the IRZ results from the balance between the irrotational axial velocity and the induced velocity w_{ind}. Changes of the flow field, provoked by Fritz and Kröner (Fritz et al. 2004; Kröner et al. 2003; Kröner et al. 2005) with the increase of the equivalence ratio or the reduction of the mixture mass flow, disturb this balance and the recirculation bubble propagates upstream. As the consequence, the flame approaches the stagnation point and the reaction zone becomes more compact. These changes cause also the generation of more negative vorticity and thus a higher induced velocity. Exceeding of a critical value initiates the sudden propagation of the bubble including the flame upstream into the premix zone and flame flashback occurs. However, flashback safe configurations as well as configurations which are prone to CIVB were identified and it was detected that even small changes of the flow field influence the stability considerably, as CIVB exhibits a high sensitivity regarding the interaction between chemistry and turbulence. The important difference between both cases was identified by numerical simulations (Kiesewetter 2005), which calculated the swirl burner experimentally analyzed before (Fritz et al. 2004). The generation of a stable and unstable burner configuration was achieved by small changes of the radial velocity profiles. The numerical simulations were able to reproduce the experimentally observed flashback limits very well and lead to an explanation of the existence of the stable and unstable cases: Stability depends on the thickness of the flame front and, most important, on the position of the flame front relative to the tip of the bubble.

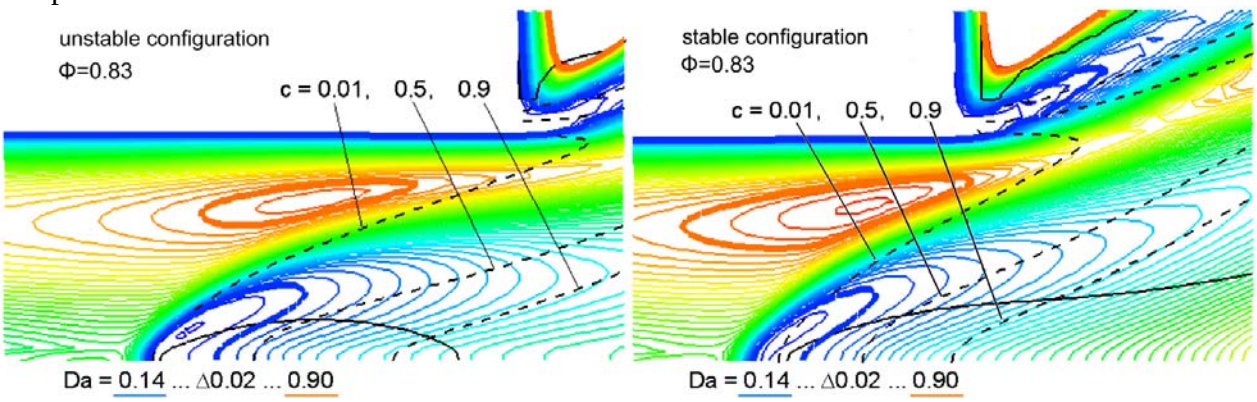

Fig. 2 Numerical comparison of the Da distribution for a safe as well as a CIVB prone configuration (Kiesewetter 2005).

Figure 2 shows a comparison of the two bubbles and the corresponding relative distribution of the Damköhler number Da. The flame itself is illustrated by dotted lines representing constant values for the progress variable c. The crucial difference between both cases is the position and extension of the reaction zone with respect to the recirculation zone. For the CIVB prone configuration the flame is more downstream of the bubble's tip due to stronger quenching in the larger zone of small Da at the bubble's forefront. The second case allows the flame to take a position more upstream due to weaker quenching resulting from the faster increasing Da in the bubble. This leads to the conclusion that the interaction between chemistry and turbulence at the bubble tip determines whether CIVB driven flashbacks occur. A more detailed view delivers the analysis of the vorticity: Although, the absolute level of production of vorticity is dominated by stretching and tilting, the changes of the vorticity budget associated with the flame are more important for the explanation of CIVB (see eq.(1)).

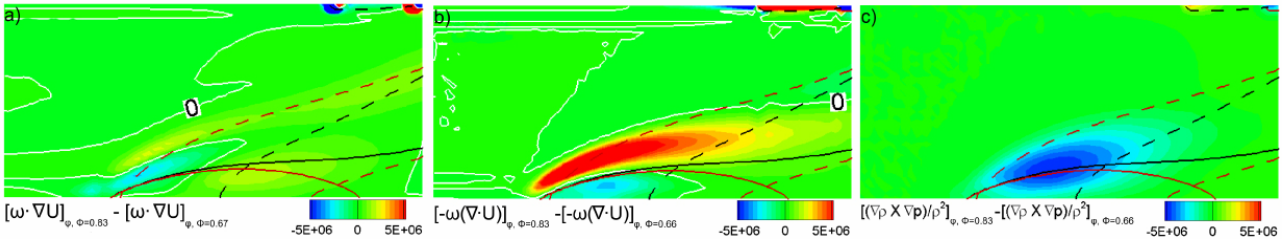

Fig. 3 Numerical calculation of the influence of the equivalence ratio on the source terms of the vorticity transport equation (stretching/tilting (a), volumetric expansion (b) and baroclinic torque (c)) (Kiesewetter 2005).

Figure 3 displays the distribution of the vorticity change due to the increase of the equivalence ratio from ϕ=0.67 to ϕ=0.83 broken down into the components stretching/tilting, volume expansion and baroclinic torque. The propagation of the bubble with the flame is the result of the increase of the induced negative axial velocity w_{ind} (eq.(2)). A thorough analysis of the flame induced vorticity changes clarifies that the volumetric expansion mainly produces positive vorticity outside and upstream of the bubble, while the baroclinic torque generates negative vorticity particularly inside the bubble. Interestingly, the influence of the flame on the vorticity change due to stretching and tilting is much smaller than these effects. Since negative azimuthal vorticity induces negative axial velocity w_{ind}, the baroclinic torque is responsible for the transition of the flame upstream and towards the final flashback, while the volumetric expansion upstream of the bubble attempts to inhibit the propagation. These findings justify the following conclusions: Only if the onset of the chemical reaction begins downstream of the stagnation point and the thickness of the reacting layer is favorable flashback will occur. In the opposite case, if the flame propagates upstream and, in the extreme case, passes the bubble tip, the heat release upstream of the recirculation zone will lead to the partial compensation of the generation of negative vorticity, which then inhibits the sudden propagation.

Figure 4 illustrates these effects. Sketch a) shows the vortex breakdown for the isothermal flow field. Due to the vortex breakdown at the cross-sectional jump of the burner exit plane a recirculation zone is created. The vorticity changes induce a force $I_{ind,isotherm}$ against the flow direction. The case with reaction is shown in b): The additional production of negative azimuthal vorticity mainly due to the baroclinic torque results in an additional force $I_{ind,baro}$, which represents additional flow resistance. Due to this effect the bubble attempts to propagate upstream until a new stable position is reached. Sketch c) shows the case of a propagating flame: After a critical value is exceeded, the flow field on the centerline loses its capability to balance the induced force, the bubble penetrates the tube and flashback occurs. However, CIVB will only occur if the flame does not get too close to the bubble tip or even passes its envelope. The sketch d) illustrates the case, when the flame has managed to reach a position upstream of the bubble tip: Because of the flame position in front of the bubble envelope and the strong heat release in this zone, the production of

positive azimuthal vorticity compensates the baroclinic torque and reduces the induced force against the main flow. Finally, this inhibits the propagation into the tube and a stable position in the combustor is retained.

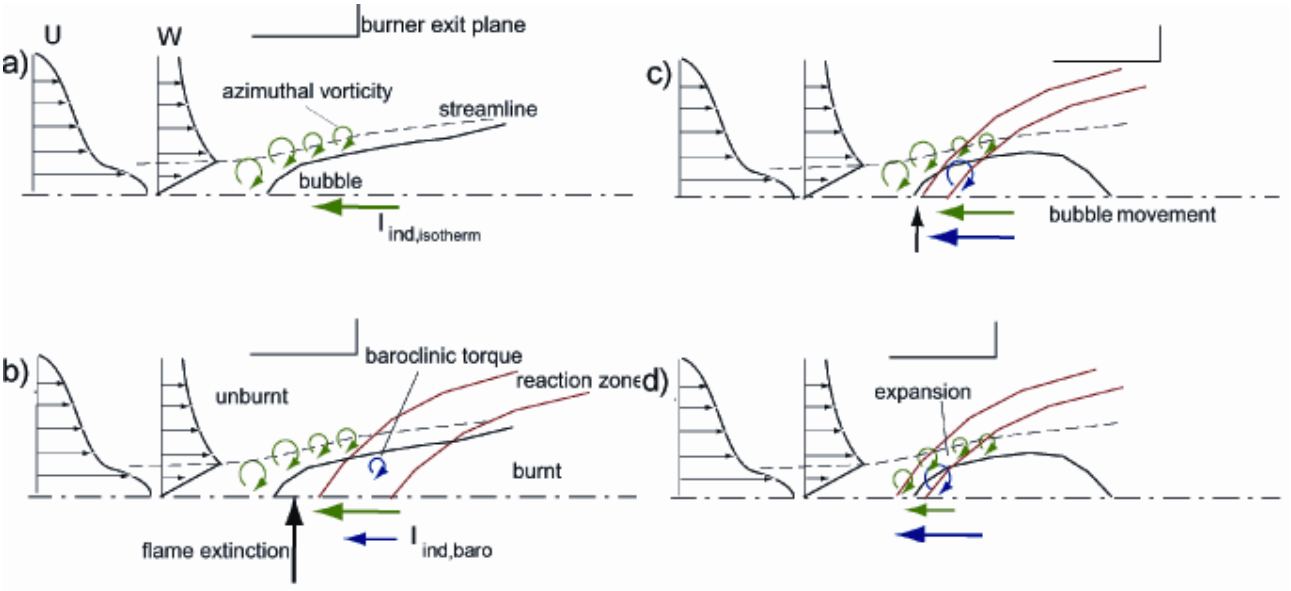

Fig. 4 The principle of the new understanding of CIVB driven flashbacks.

In summary, the numerical calculations (URANS) have lead to a substantial improvement of the understanding of CIVB driven flame flashback. Proving that it is really valid requires the validation of the assumption that the occurrence of CIVB is governed by the relative position of the flame front and the recirculation bubble. The motivation for the experimental investigations presented below is the validation of this assumption. For this purpose a burner geometry is employed, which is considerable different to the configuration in the CFD study, in order to show that the assumption is generally valid.

3. Experimental Setup

The experimental studies were carried out using a modular and flexible swirl burner system without centerbody (Burmberger et al. 2006). This burner operates in externally premixed mode. A static mixer is implemented upstream in order to avoid any equivalence ratio fluctuations. Figure 5 displays the burner. The main flow passes a swirl generator and stabilizes the flame by vortex breakdown near the burner exit plane. The position of the vortex breakdown is optimized with an additional unswirled core flow. This axial jet passes three sequentially mounted perforated plates for an additional pressure loss. The fraction of the center flow is maximum 30% vol. of the total flow. The burner nozzle has an inner diameter of D = 40mm. Figure 6 shows a stability map to characterize the burner. The core flow limit, at which CIVB occurs, is plotted via thermal power for a constant equivalence ratio of 1. The curve shows the trend that the higher thermal power is, the more the stabilizing core flow can be reduced without the occurrence of flashback.

While Fritz and Kröner (Fritz et al. 2004; Kröner et al. 2003; Kröner et al. 2005) initialized flashbacks by increasing the equivalence ratio, the unswirled core flow was used to trigger CIVB for the measurements described below. To allow optical accessibility for the lasers as well as for the detection systems a transparent mixing tube with the same inner diameter of D = 40 mm as the exit nozzle was installed (fig. 5). The tube had a length of three diameters D and was made of silica glass to allow transmission of all required wavelengths, especially UV light for LIF.

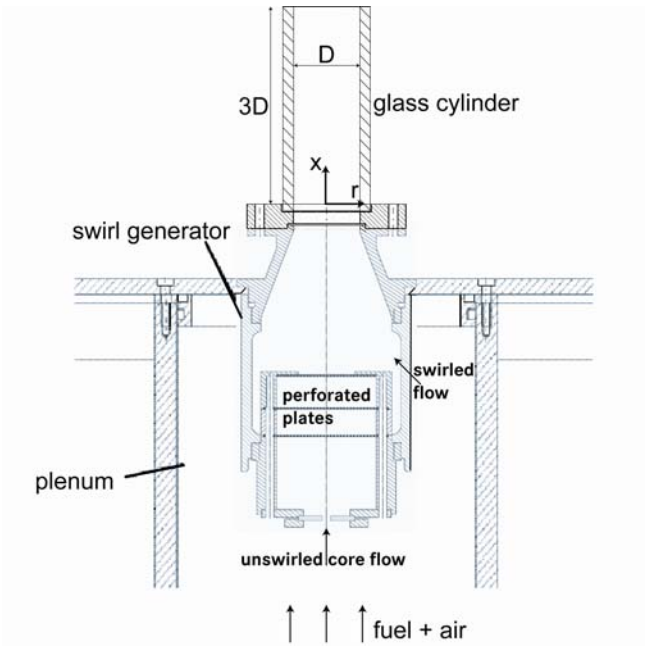

Fig. 5 Sketch of the investigated burner system

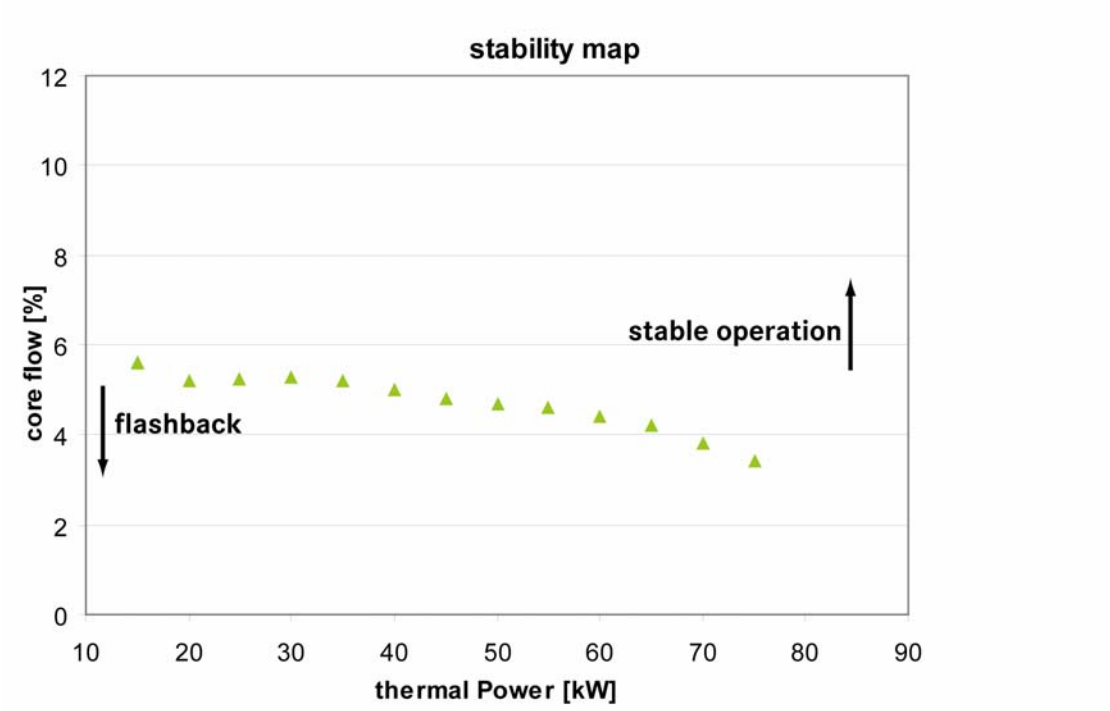

Fig. 6 Stability map of the investigated swirl burner

4. Measurement Techniques

A proper analysis of the interaction between turbulence and chemistry requires that the dynamical behavior of the flame front is identified and that the dynamic changes of the velocity field during flashback are measured simultaneously. Therefore, the laser induced fluorescence is implemented to track the flame front and the particle image velocimetry is used to visualize the flow. In the following sections the used systems will be presented and image processing procedures for the analysis of the recorded data will also be explained.

4.1. Laser Induced Fluorescence

The detection of the flame front is accomplished with Planar Laser Induced Fluorescence (HS-PLIF). LIF reveals the boundary between the unburned premixed gas and the burnt gas, which appears in form of a sudden increase of the OH concentration (Eckbreth 1996). The excitation of this combustion intermediate is achieved with a Nd:YAG pump laser, combined with a dye laser operated with Rhodamine 6G and a frequency doubler. OH is excited with a wavelength of 283nm, a pulse energy of 80μJ and a repetition rate of 1000Hz. The light sheet, which illuminates a height of 2 D (D = diameter of the mixing tube), is generated using the combination of a cylindrical and a spherical lens. The detection system for the UV fluorescence signal is a high speed camera with integrated fiber optical coupled intensifier. The memory size of the camera allows the recording of two seconds with the maximum spatial resolution of 1024x1024 pixels. In the experiments, a field of view of 162.5mm x 162.5mm was selected. The camera lens has a focal length of 45mm and an aperture of 1:1.8. For the suppression of disturbing scattered light a UV high pass filter is used with a transmission of 80% at the fluorescence wavelength around 308nm. This scattered light occurs mainly due to the reflections of the LIF laser pulse at the PIV particles.

The necessary post-processing procedures were accomplished with Matlab and its Image Processing Toolbox. Since reflections at the glass cylinder cannot be completely avoided by apertures and also not completely suppressed by setting detection thresholds, these disturbing signals had to be eliminated by the subtraction of a background image. In the next step the sudden increase of the OH concentration was identified by the detection of the highest gray value gradients of the LIF images.

4.2. Particle Image Velocimetry

The velocity field within the flame is acquired with Particle Image Velocimetry (HS-PIV), which observes the streamlines of particles injected into the reacting flow. This requires a second light sheet and a double pulse technique. For this purpose, a Nd:YLF laser with two cavities was applied. The emitted light has a wavelength of 527nm and a pulse energy of 10mJ. In the study, the light sheet had a width of 2mm on the burner centerline and a height similar to the LIF light sheet. The temporal separation of the double pulses was 30μs. The detection system for the elastic scattering is a high speed camera. The synchronization between the camera and the light pulses is displayed in Figure 7 (right hand side). The camera memory allows the investigation of one second with maximum spatial resolution of 1024x1024 pixels and a recording frequency of 2000Hz. The distance between the camera and the illuminated plane was adjusted to deliver a field of view of 106mm x 106mm. The camera lens has a focal length of 85mm with an aperture of 1:1.4. In order to block disturbing signals an interference filter for 532nm is mounted in front of the camera CMOS sensor. The filter provides 90% transmission and has a half-power bandwidth of $\pm$10nm. The captured PIV double frames were analyzed with interrogation areas of 32x32 pixels using an adaptive cross-correlation with 50% overlapping. Thus, the spacing between the calculated velocity vectors is 1.65mm. TiO_2 particles are used due to their high temperature-resistance.

The calculation of the velocity information is done with the software VidPIV (Intelligent Laser Applications GmbH 2004) and with post-processing procedures programmed in Matlab. Light scattering at the glass cylinder surface is eliminated by background subtraction. After the calculation of the velocity the data is transferred in Matlab data format to display the flow field with the flame front recorded with LIF simultaneously.

4.3. Synchronization

Figure 7 shows the setup of the measurement techniques and the triggering scheme. The cameras are positioned vis-à-vis and the lasers emit both in the same direction. The two superimposed light sheets penetrate the burner center at right angle to both detection systems. For the synchronization of both techniques, the LIF laser diode pulse is chosen as the master signal. Symmetrically to this master signal the two PIV laser cavities emit their pulses. To protect the LIF detection system against overexposure, the LIF camera intensifier is activated between the PIV laser pulses. (fig. 7, right hand side).

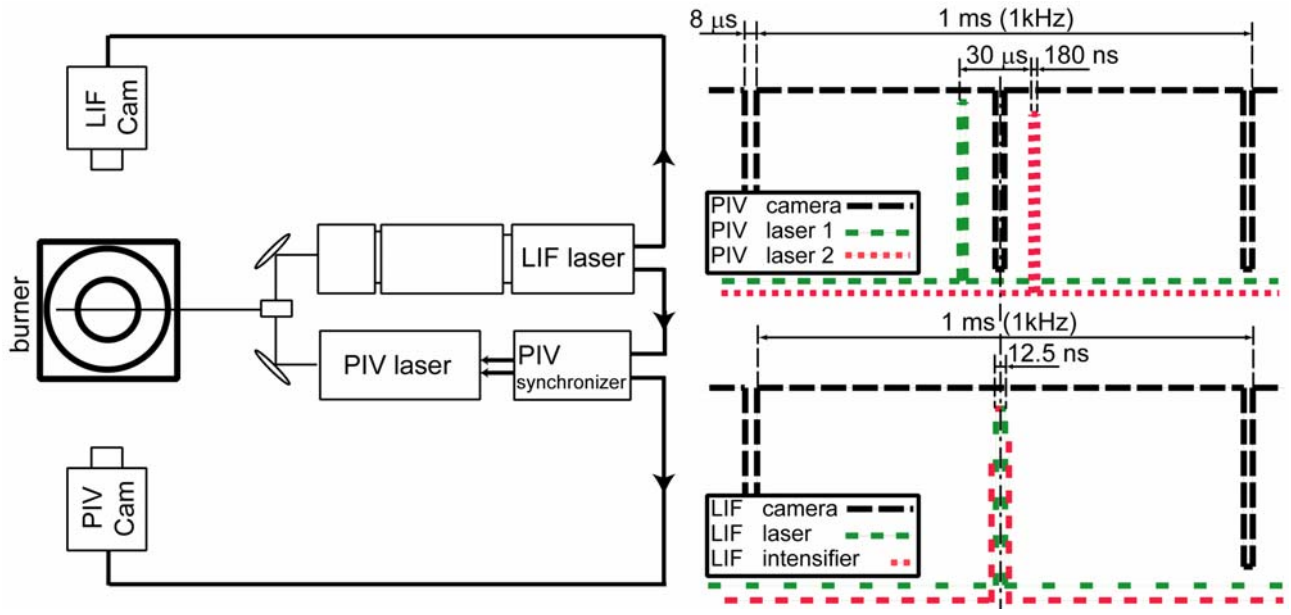

Fig. 7 Sketch of the setup and the triggering scheme

5. Results

Figure 8 shows the velocity field (vectors) as well as the flame contour (gray line) measured simultaneously. The operating point for this image was $P_{thermal}$ = 30kW, Φ = 0.83 and the core flow was set to 10%. The location of the vortex tube is also illustrated. The envelope of the bubble is displayed with a dotted line. For this operating point the position of the flame contour is approximately 0.1 D downstream of the tip of the bubble.

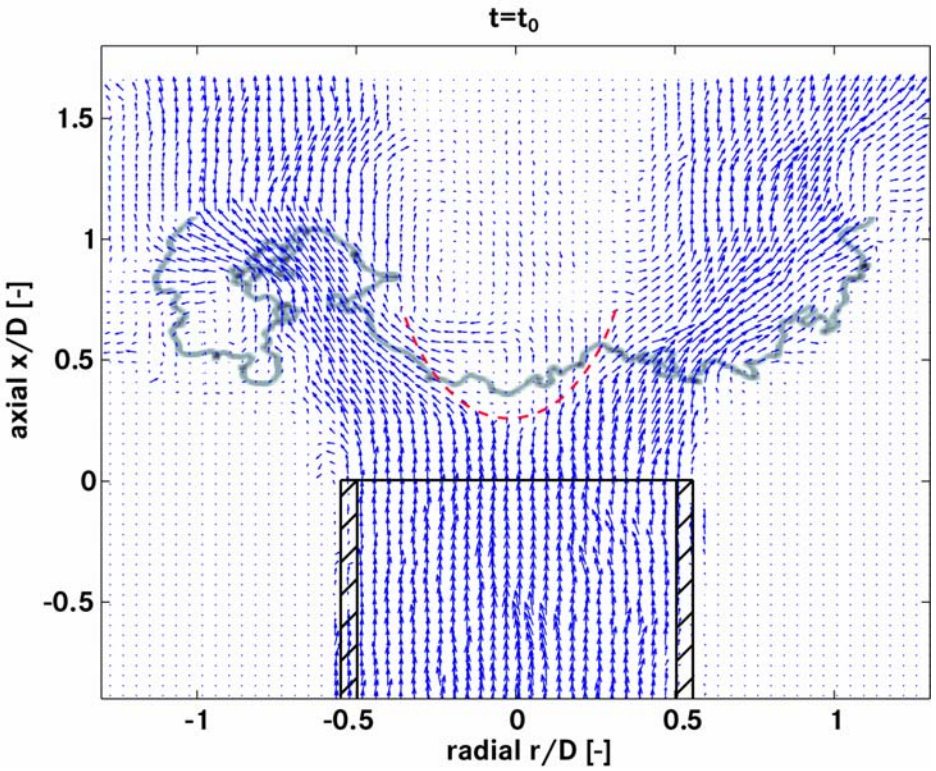

Fig. 8 Flame front (gray line) and velocity field (vectors); the bubble envelope is shown with a dotted curve

Figure 9 displays close-up views of the tip of the bubble taken within 6ms after recording of figure 8. Again, the bubble envelope is marked with a dotted line. While during the first three shots the bubble is displaced downstream, the flame moves against the flow direction and passes even the tip of the bubble. 3ms are required before the bubble reaches its starting position at t_0 again and the flame is then shifted to a position further downstream. The explanation of this effect is that the sudden propagation of the flame upstream initializes a higher volume expansion upstream the tip of the bubble and therefore positive vorticity changes (eq.(1)). The consequence is the reduction of the induced velocity w_{ind} (eq.(2)) against the main flow and the displacement of the bubble downstream. Since the flame is bound to the bubble as flame holder, the flame follows the bubble movement with some delay. In the next phase, the motion of the flame downstream with respect to the bubble position reduces the vorticity changes again, the induced force increases and the bubble reaches again its starting position (fig. 9, $t = t_0+6ms$).

The investigated operating point shows the stochastic character of the onset of CIVB. In this transitional regime the movement of the flame with respect to the bubble is small. However, this disturbance initiates changes of the vorticity and as consequence the displacement of the stable bubble position occurs. Crucial for the subsequent macroscopic propagation of the bubble with the flame is the interaction between volume expansion and baroclinic torque. If volume expansion due to the additional heat release dominates the vorticity changes, the sudden upstream propagation is inhibited. The configuration analyzed in fig. 9 shows this case. Once the baroclinic torque overcompensates the increase of vorticity changes due to volume expansion and the generation of negative vorticity begins to dominate, CIVB driven flashback occurs. Thus, CIVB safe configurations exhibit a balance of positive vorticity due to volume expansion and negative vorticity generated by baroclinic torque. Only in CIVB prone cases this balance is finally lost in the region of the bubble tip and the flame is able to propagate with the bubble upstream through the cylindrical part of the burner.

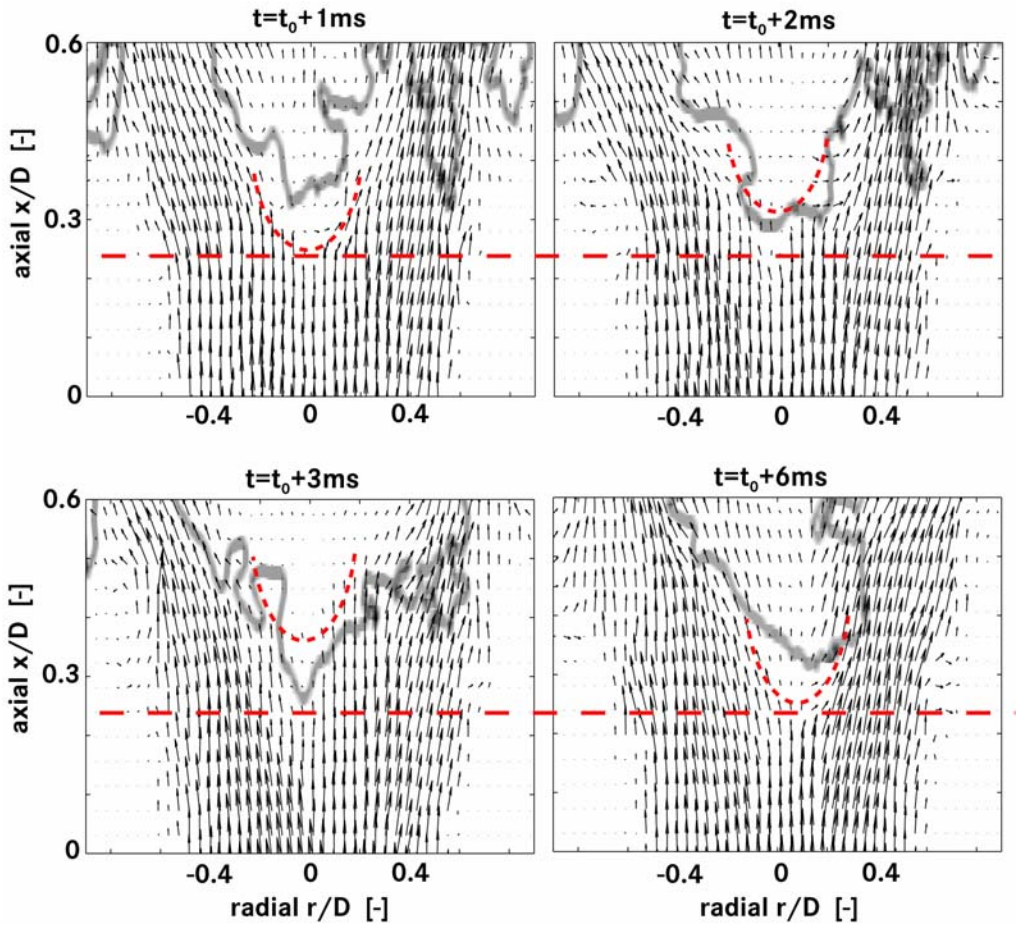

Fig. 9 Behavior of the bubble during flame propagation

In Figure 10 the influence of the core flow is illustrated. The reduction of the core flow from 10% to 5.5% volume fraction leads to the displacement of the bubble 0.4 D upstream. The stability map (fig. 6) showed that the operating point with 5.5% core flow is at the flashback limit. The bubble has already a position inside the mixing tube. A further reduction of the stabilizing axial jet will lead to the propagation of the flame through the mixing tube into the swirl generator.

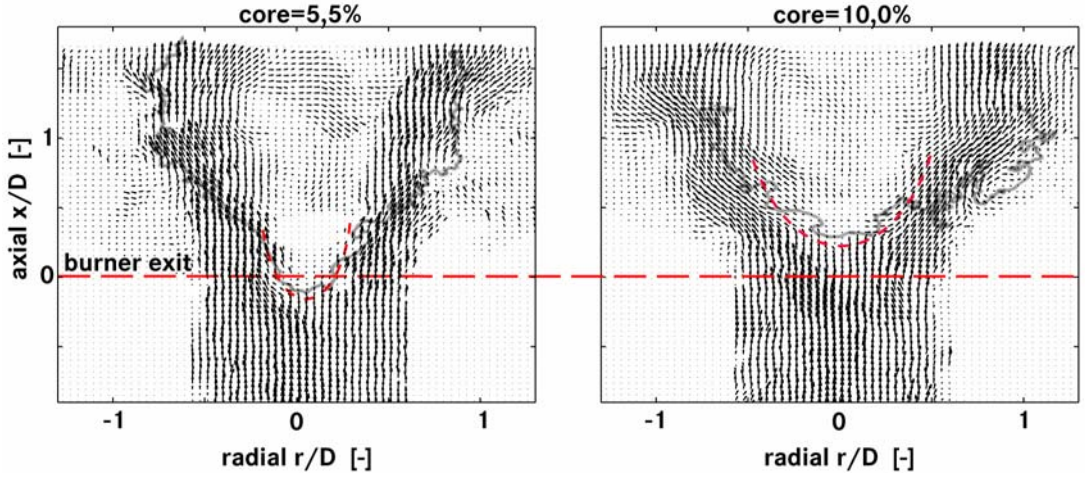

Fig. 10 Influence of the core flow on the bubble position

6. Conclusions and Outlook

With the simultaneous high-speed PIV and LIF measurements near the onset of CIVB driven flashback the interaction between flame and recirculation bubble was investigated with high temporal resolution. From the study, the following conclusions can be derived:

- The analysis of the flame position with respect to the bubble tip confirms the results of earlier CFD-studies (Kiesewetter 2005), although the numerical findings were derived from URANS computations (fig. 3), which did not provide true temporal resolution like the experiments.
- The occurrence of CIVB driven flashback is governed by the interaction of turbulence and chemistry at the tip of the recirculation bubble, which govern the vorticity generation in the reaction zone.
- The flame position with respect to the bubble influences the net vorticity generation due to volume expansion and baroclinic torque.
- Before CIVB driven flashback occurs a transitional regime with highly stochastic upstream propagation of the flame with respect to the bubble is observed.
- The total induced force against the flow direction has to exceed a threshold before CIVB driven flashback occurs. As long as the baroclinic torque is not able to dominate over the stabilizing contribution of the heat release, flashback is inhibited.
- Since the geometry of the investigated swirl burner differs substantially from the burner analyzed experimentally by (Fritz et al. 2004; Kröner et al. 2003; Kröner et al. 2005) and numerically by (Kiesewetter 2005) before, there is evidence that the observed effects are not limited to one specific burner geometry.

In the near future, the current experimental work will be extended to the investigation of the influence of the mixture temperature and the vortex core radius. Furthermore, numerical simulations of the investigated burner will be made and the methodology will be refined to cover the stochastic effects.

Acknowledgements

The authors gratefully acknowledge the financial support by the Bavarian Research Cooperation (FortVer) and the German Research Council (DFG) through the Research Unit „Combustion Induced Vortex Breakdown“.

References

Burmberger S., Hirsch C., Sattelmayer T., *Designing a Radial Swirler Vortex Breakdown Burner*, Proceedings of ASME Turbo Expo, Barcelona, Spain, 2006.

Darmofal D. L., *The Role of Vorticity Dynamics in Vortex Breakdown*, AIAA Paper 93-3036, 24th Fluid Dynamic Conference, 1993.

Eckbreth A.C., *Laser Diagnostics for Common Combustion Temperature and Species*, Combustion Science & Technology Book Series, Volume 3, 1996.

Fritz J., Kröner M., Sattelmayer T., *Flashback in a Swirl Burner With Cylindrical Premixing Zone*, Journal of Engineering for Gas Turbines and Power, 126:276-283, 2004.

Hasegawa T., Nishiki S., Michikami S., *Mechanism of Flame Propagation along a Vortex Tube*, IUTAM Symposium on Geometry and Statistics of Turbulence, 235-240, Kluwer Academic Publisher, 2001.

Intelligent Laser Applications GmbH, *VidPIV 4.6 Particle Image Velocimetry Software Brochure*, Jülich, Germany, 2004.

Kiesewetter F., Hirsch C., Fritz J., Kröner M., Sattelmayer T., *Two-Dimensional Flashback Simulation in Strongly Swirling Flows*, Proceedings of ASME Turbo Expo, Atlanta, USA, 2003.

Kiesewetter F., *Modellierung des verbrennungsinduzierten Wirbelaufplatzens in Vormischbrennern*, Dissertation, TU München, 2005.

Kröner M., Fritz J., Sattelmayer T., *Flashback Limits for Combustion Induced Vortex Breakdown in a Swirl Burner*, Journal of Engineering for Gas Turbines and Power, 125:693-700, 2003.

Kröner M., Sattelmayer T., Fritz J., Kiesewetter F., Hirsch C., *Flame Propagation in Swirling Flows - Effect of Local Extinction on the Combustion Induced Vortex Breakdown*, Draft for Combustion Science and Technology, 2005.

Panton R. L. *Incompressible Flow*, Wiley Interscience, 1996.